

NASA CONTRACTOR
REPORT

NASA CR-129015

(NASA-CR-129015) SCATTERING FROM
CONDENSATES IN TURBULENT JETS Final
Report (IIT Research Inst.) 35 p HC
\$3.75

CSCI 20D

N74-12088

Unclas
G3/12 23599

SCATTERING FROM CONDENSATES
IN TURBULENT JETS

By L. N. Wilson and R. S. Dennen
Engineering Mechanics Division
IIT Research Institute
10 West 35th Street
Chicago, Illinois 60616

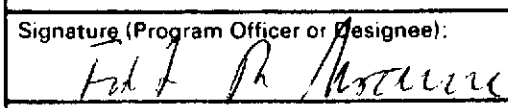
April 28, 1970

Final Report



Prepared for

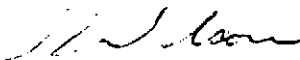
NASA-GEORGE C. MARSHALL SPACE FLIGHT CENTER
Marshall Space Flight Center, Alabama 35812

1. REPORT NO. NASA CR-129015		2. GOVERNMENT ACCESSION NO.		3. RECIPIENT'S CATALOG NO.	
4. TITLE AND SUBTITLE SCATTERING FROM CONDENSATES IN TURBULENT JETS				5. REPORT DATE April 28, 1970	
				6. PERFORMING ORGANIZATION CODE	
7. AUTHOR(S) L. N. Wilson and R. S. Dennen				8. PERFORMING ORGANIZATION REPORT # J6112 Part III	
9. PERFORMING ORGANIZATION NAME AND ADDRESS Engineering Mechanics Division IIT Research Institute 10 West 35th Street Chicago, Illinois 60616				10. WORK UNIT NO.	
				11. CONTRACT OR GRANT NO. NAS 8-21035	
12. SPONSORING AGENCY NAME AND ADDRESS National Aeronautics and Space Administration Washington, D. C. 20546				13. TYPE OF REPORT & PERIOD COVERED High Series Contractor Final	
				14. SPONSORING AGENCY CODE	
15. SUPPLEMENTARY NOTES					
16. ABSTRACT					
<p>An analysis is made of the scattering signal levels to be expected from condensed water vapor droplets for crossed-beam instruments operating in the wavelength region $.18\mu$ to 4.3μ. The results show that scattering should not present a problem for the infra-red system operating under conditions typical of the IITRI jet facility. Actual measurements made for comparison indicate that scattering levels are appreciable, and presumably result from oil mist added by the facility air compressors.</p>					
17. KEY WORDS			18. DISTRIBUTION STATEMENT Unclassified-unlimited		
			Signature (Program Officer or Designee): 		
19. SECURITY CLASSIF. (of this report) Unclassified		20. SECURITY CLASSIF. (of this page) Unclassified		21. NO. OF PAGES 33	
				22. PRICE NTIS	

FOREWORD


This report was prepared by the IIT Research Institute for the National Aeronautics and Space Administration Marshall Space Flight Center, on Contract No. NAS8-21035. The effort described here constitutes the scattering and absorption study, which is part of the cross-beam system development. This report includes an assessment of the effects of scattering from water vapor condensate and the ability of the infra-red system to discriminate against them. The development of the infra-red system and its application to sound-source measurements are described in separate reports. The personnel who have contributed to this report include: R. J. Damkevala and M. Phillips.

Respectfully submitted,
IIT RESEARCH INSTITUTE



L. N. Wilson
Manager
Fluid Dynamics & Acoustics

APPROVED BY:



M. R. Johnson
Assistant Director
Engineering Mechanics Division
/mer

CONTENTS

<u>Section</u>	<u>Page</u>
I. INTRODUCTION	1
II. DEVELOPMENT OF THE SCATTERING MODEL	2
A. Scattering Processes	2
B. Condensation Mechanism	3
C. Particle Size Distribution	6
D. Scattering Signal Determination	8
III. COMPUTATION OF SCATTERING SIGNAL	10
A. Computer Program	10
B. Limiting Solutions	12
1. Optical Region	12
2. Rayleigh Region	13
C. A Sample Problem	14
D. Extrapolation to Other Flow Conditions	17
IV. EXPERIMENTAL STUDIES	18
A. Relation of Measured Signals to Mean Extinction	18
B. Observations	20
V. DISCUSSION	22
REFERENCES	

SCATTERING FROM CONDENSATES IN TURBULENT JETS

I. INTRODUCTION

Measurements⁽¹⁾ of turbulent intensities in supersonic jets, using an ultra-violet, crossed-beam system appeared to give a signal which originated in scattering of light from condensed water vapor or some other condensate, rather than in the absorption of light by O_2 molecules. Further measurements with a He-Ne laser crossed-beam instrument⁽²⁾ substantiated this observation. It was in part this uncertainty about the origin of the signals, that led to the development of an infra-red crossed-beam system. The infra-red system has the advantage of the ultra-violet system in that it is sensitive to a naturally-occurring air specie (CO_2 rather than O_2) but also it operates at a more favorable wavelength for the suppression of scattering. Whether or not a real gain is realized, however, depends upon the relative levels of scattering and absorption signals. It is the purpose of the study reported here to develop a mathematical model for scattering from condensates and to apply the results to assess the contribution of scattering from condensed water droplets in the wavelength region of the CO_2 (4.3μ) vibration band.

II. DEVELOPMENT OF THE SCATTERING MODEL

A. Scattering Processes

Light scattering from particles results from the interaction between the electric field of the light wave and the electric dipole moment (either permanent or induced) in the particle. The effectiveness of a particle as a scatterer is described by its scattering cross-section K , which is the ratio of the effective cross-sectional area of the particle in reducing the incident light intensity, to its actual cross-sectional area. K is dependent not only upon the optical properties of the particle, but also the ratio of particle radius (a) to wavelength (λ), in the form $\alpha = \frac{2\pi a}{\lambda}$. There are three general regions of scattering determined by the value of α :⁽³⁾

- 1) Rayleigh scattering region
- 2) Mie scattering region
- 3) Optical region

In the Rayleigh region $\alpha \rightarrow 0$, and the particle size is much smaller than the wavelength, (an example is scattering from air molecules). In this case K increases rapidly with α , behaving like α^4 at $\alpha = 0$. In the Mie region, the particle size becomes comparable with the wavelength and interference between the incident light and the scattered light results in a value of K which generally oscillates about a mean as α

increases. In the Optical region the particle is much larger than the wavelength and the laws of Geometrical Optics hold. The shape of the K vs α scattering curve for forward scattering from spherical water droplets is reproduced from reference 4 in Figure 1, and is typical in shape of those for most other materials.

Light which is scattered from one particle may be rescattered from a second particle. The cross-sections for this multiple scattering are much smaller than those for single scattering and will be ignored here.

For single scattering we can write, using the definition of K ;

$$\frac{dI}{I dx} = - \pi \int_0^{\infty} K(\alpha) a^2 dN'(a) \quad (1)$$

where I is the intensity of the light beam,

x is distance along the beam, and

$dN'(a)$ is the number of scattering particles of radius between a and $a + da$ per unit of length along x .

This equation will serve as the basis for the scattering estimates.

B. Condensation Mechanism

Liquid and solid condensates, such as water droplets or ice crystals can be formed in an unheated air jet when it expands to a temperature which is below either the dew point of the jet air or the surrounding ambient air. The latter case becomes important where the jet air is dried to a very low

dew point. Then the ambient, wet air is entrained into the jet by turbulent mixing and is cooled by conduction of heat to the jet air. At sufficiently low temperatures (high jet Mach numbers) the condensed water droplets thus formed may freeze into ice crystals. At still lower temperatures, CO_2 or even O_2 and N_2 in the air may condense to form solid crystals. The dominant scattering specie, therefore is determined by the jet operating conditions of stagnation temperature and Mach number.

The dynamics of the formation of solid or liquid condensate particles are extremely complex, since the particles do not form instantaneously once the dew or freezing points are reached, i.e. some degree of supersaturation always occurs. However, if formation is delayed by supersaturation the result will be fewer particles being formed at a given downstream location in the jet. The net result of assuming no supersaturation then, will always ensure we do not underestimate the total number. Another complication occurs in attempting to describe the spatial distribution of particles in the turbulent jet. The mechanism of mixing by turbulence is a complicated one, and in fact its study is one of the basic objectives of crossed-beam studies. A further, and again "safe", simplification will therefore be made with respect to mixing of the condensed particles. It will be assumed that the particles are uniformly mixed throughout that portion of the jet which is below dew point. The validity of this assumption improves with increasing downstream locations.

If the beam passes through a length L where the temperature is below dew point and the beam diameter is d , there is a volume of gas

$$V = \frac{\pi d^2 L}{4} \quad (2)$$

within the beam at any instant of time. If the partial pressure of condensible vapor is $P_v(T_a) \equiv P_{va}$ before being cooled (temperature T_a) and is $P_v(T_j) \equiv P_{vj}$ after being cooled, (temperature T_j) then the mole fraction of condensate lost is $\frac{P_{va}}{P_a} - \frac{P_{vj}}{P_a} \frac{T_a}{T_j}$ where P_a is the partial pressure of air and is assumed equal to the jet (or ambient) pressure. Latent heat added by the condensing processes is assumed to be small, and not to affect the jet temperature. Also, T_j should be the average temperature in the jet at the downstream location of the beam. The ratio of total mass of condensible vapor to total mass of air is therefore

$$\frac{m_v}{m_a} = \frac{M_v}{M_a} \frac{P_{va}}{P_a} \left(1 - \frac{P_{vj}}{P_{va}} \frac{T_a}{T_j} \right) \quad (3)$$

where M_v , M_a are the molecular weight of vapor and air
 $P_{vj} = P_{sj}$ is the saturation partial pressure at temperature T_j .

Having calculated the total mass of condensible vapor it is necessary, in order to determine scattering effects to estimate particle size distribution. The common probability distribution functions (e.g. Gaussian) will not suffice here since they allow a finite number to exist at zero and negative sizes. A well behaved distribution for our purposes is a Gamma distribution and this is discussed in the following section.

C. Particle Size Distribution

The Gamma probability distribution has the form⁽⁵⁾

$$p(a) = A a^n e^{-ma} \quad (4)$$

There are several conditions placed upon equation (4) which determine the parameters A, n, m. These are

$$1. \int_0^{\infty} p(a) da = 1$$

$$2. \int_0^{\infty} p(a) a da = a_m = \text{mean particle radius}$$

$$3. \int_0^{\infty} p(a) (a - a_m)^2 da = \langle (a - a_m)^2 \rangle = \frac{a_m^2}{\sigma^2}$$

The shape variable σ is defined by $\frac{1}{\sigma^2} = \frac{\langle (a - a_m)^2 \rangle}{a_m^2}$

Using these conditions we obtain

$$1. A = \frac{(\sigma/a_m)^\sigma}{\Gamma(\sigma)}$$

$$2. m = \frac{\sigma}{a_m}$$

$$3. n = \sigma - 1$$

$$\text{or } p(a) = \frac{\sigma}{\Gamma(\sigma)} \left(\frac{\sigma a}{a_m} \right)^{\sigma-1} \frac{e}{a_m} - \left(\frac{\sigma a}{a_m} \right) = \frac{1}{N} \frac{dN(a)}{da} \quad (5)$$

Figure 2 show some plots of $p(a)$ for $\sigma = 4, 8, 16, 24, 36, \infty$ and $a_m = 2\mu$. In the limit $\sigma \rightarrow \infty$ equation (5) defines a δ -functional, the particular case where all particles are of the same size a_m . Since $p(a) da = \frac{dN}{N}$ we see that the mean

particle size and dispersion of particle sizes are easily controlled independently through a_m and σ . Using equations 2, 3 and 5 we can now estimate the total number of particles and their distribution.

The volume of each particle of condensate is $\frac{4}{3} \pi a^3$ and its mass is $\frac{4}{3} \pi a^3 \rho_c$. The total mass m_c of condensate of N particles distributed about a mean size a_m according to equation 5 then is

$$\begin{aligned} m_c &= \int_0^{\infty} \frac{4}{3} \pi \rho_c a^3 dN = \frac{4}{3} \pi \rho_c N \int_0^{\infty} a^3 p(a) da \\ &= \frac{4}{3} \pi N \rho_c \frac{\sigma}{\Gamma(\sigma)} \int_0^{\infty} \left(\frac{\sigma a}{a_m} \right)^{\sigma-1} \frac{a^3}{a_m} e^{-\frac{\sigma a}{a_m}} da \\ &= \frac{4}{3} \pi a_m^3 \rho_c \frac{(\sigma+2)(\sigma+1)N}{\sigma^2} \end{aligned} \quad (6)$$

Now $m_c = m_v$, the mass of vapor which could be present without condensation, and letting $m_a = \rho_a V = \rho_a \pi d^2 L$ we obtain from equations (3) and (6),

$$N = \frac{3}{16} \frac{d^2 L}{a_m^3} \frac{M_v}{M_a} \frac{P_{sa}}{P_a} \left(\beta - \frac{P_{sj}}{P_{sa}} \frac{T_a}{T_j} \right) \frac{\rho_a}{\rho_{cj}} \frac{\sigma^2}{(\sigma+1)(\sigma+2)} \quad (7)$$

Here we have assumed the jet saturated so that $P_{vj} = P_{sa}$ and that the relative humidity of the ambient air $\frac{P_{va}}{P_{sa}} = \beta$

Equations (5) and (7) thus allow the determination of particle numbers and sizes. It now remains only to calculate the scattered signal using equation (1).

D. Scattering Signal Determination

Using Equation (1) we can integrate to obtain

$$\ln I = - \int_0^{\infty} \int_0^{\infty} K(\alpha) \pi a^2 d N'(a) dx$$

If a is taken independent of x , i.e. particles are uniformly distributed within the beam, then

$$\begin{aligned} \ln I &= - \pi \int K(\alpha) a^2 d N'(a) L \\ &= - \pi \int K(\alpha) a^2 d N(a) \\ &= - \pi N \int K(\alpha) a^2 p(a) da \\ &= - \pi K_{\text{eff}}(\alpha_m) a_m^2 N \end{aligned}$$

$$\text{or} \quad \frac{I}{I_0} = \exp - \left\{ K_{\text{eff}}(\alpha_m) a_m^2 N \right\} \quad (8)$$

$$\text{where} \quad K_{\text{eff}}(\alpha_m) = \int_0^{\infty} K(\alpha) \left(\frac{a}{a_m} \right)^2 p(a) da \quad (9)$$

We note that for $\sigma = \infty$, $p(a) = \delta(a - a_m)$
and $K_{\text{eff}} = K(\alpha_m)$.

The total number of particles is a function of the dispersion in particle sizes through the factor $\frac{(\sigma + 1)(\sigma + 2)}{\sigma^2}$

For $\sigma = \infty$, this factor is unity, increasing to 6 for $\sigma = 1$.

In review then, the pertinent equations for the determination of light extinction by scattering from condensates are as follows:

$$\frac{I}{I_0} = \exp \left\{ - \pi K_{\text{eff}}(\lambda) a_m^2 N \right\} \quad (8)$$

$$N = \frac{3}{16} \frac{d_L^2}{a_m^3} \frac{M_v}{M_a} \frac{P_{sa}}{P_a} \left(\beta - \frac{P_{sj}}{P_{sa}} \frac{T_a}{T_j} \right) \frac{\rho_a}{\rho_{cj}} \frac{\sigma^2}{(\sigma+1)(\sigma+2)} \quad (10)$$

$$K_{\text{eff}}(\alpha_m) = \int_0^\infty K(\alpha) \left(\frac{a}{a_m} \right)^2 p(a) da \quad (9)$$

$$p(a) = \frac{\sigma}{\Gamma(\sigma)} \left(\frac{\sigma a}{a_m} \right)^{\sigma-1} \frac{\exp - \left(\frac{\sigma a}{a_m} \right)}{a_m} \quad (5)$$

Restricted by the following assumptions:

1. No supersaturation
2. Uniform spatial distribution of particles
3. Gamma distribution of particle sizes
4. Uniform temperature in jet where saturation occurs.

III. COMPUTATION OF SCATTERING SIGNAL

A. Computer Program

Equations 5, 8, 9 and 10 comprise the equations necessary to calculate expected scattering through a jet with condensing vapors. They apply obviously only to mean scattering, consideration of the turbulent statistics is left to a following section. The solution to the equations is straight-forward using numerical techniques, and a program has been written in Fortran IV for the determination of scattering levels.

Input constants required are as follows:

d	beam diameter
L	effective path length within the jet
λ	wavelength
a_m	mean particle size
σ	inverse of dispersion in particle size
M_v	molecular weight of vapor
M_a	molecular weight of air
ρ_{cj}	density of condensate at jet temperature
ρ_a	density of condensate at air temperature
β	relative humidity of inlet air
P_a	pressure of ambient air
P_{sa}	vapor saturation pressure at ambient air temperature
P_{sj}	vapor saturation pressure at jet temperature
$K(\alpha)$	scattering cross-section

The material properties are all obtainable from handbooks (e.g. reference 6). The scattering cross-section $K(\alpha)$ can be found tabulated in a variety of texts (e.g. reference 7). The humidity of the inlet air β must be measured or at least estimated. This leaves the particle sizes, as characterized by a_m and σ as the main unknown inputs. Only educated guesses can be made of the likely ranges of these parameters and then, by performing calculations, the sensitivity of the results to variations in the parameters can be determined. Such calculations are reported in a later section.

B. Limiting Solutions

Although in general, the integral for K_{eff} in equation 9 cannot be solved directly and we must resort to numerical solution, there are particular cases where direct, closed-form solutions can be found. Of these, two limiting cases are of importance to us, viz., the Rayleigh region and the Optical region, where we can substitute analytical forms for $K(\alpha)$.

1. Optical Region

The simplest of the two is the optical region where $K(\alpha) = K_0 = \text{const.}$

Then equation 9 becomes

$$K_{\text{eff}} = K_0 \int_0^{\infty} \left(\frac{a}{a_m}\right)^2 p(a) da$$

Using equation 5, for $p(a)$ this becomes

$$K_{\text{eff}} = K_0 \frac{\sigma + 1}{\sigma} \quad (11)$$

Rather than give the complete form for $\frac{\Delta I}{I_0}$ here, we will determine the ratio for a general value of σ to that for $\sigma = \infty$, that is $\frac{\Delta I_{\sigma}}{\Delta I_{\delta}}$. Further let us assume (although this is not necessary, and is done only for convenience) that the exponent of equation 8 is sufficiently small that we can write

$$\frac{\Delta I}{I_0} = \pi K_{\text{eff}} a_m^2 N \quad (12)$$

$$\text{Then } \frac{\Delta I}{\Delta I_{\delta}} = \frac{(K_{\text{eff}})_{\sigma} N}{(K_{\text{eff}})_{\delta} N_{\delta}} \quad (13)$$

From equation 11,

$$\frac{(K_{\text{eff}})_{\sigma}}{(K_{\text{eff}})_{\delta}} = \frac{\sigma + 1}{\sigma} \quad (14)$$

and from equation 10

$$\frac{N_{\sigma}}{N_{\delta}} = \frac{\sigma^2}{(\sigma + 2)(\sigma + 1)} \quad (15)$$

Using equations 14 and 15 with 13,

$$\frac{\Delta I_{\sigma}}{\Delta I_{\delta}} = \frac{\sigma}{\sigma + 2} \quad (16)$$

As an example, for $\infty > \sigma > 4, 1 > \frac{\Delta I_{\sigma}}{\Delta I_{\delta}} > \frac{2}{3}$

representing a rather small error involved in ignoring the particle size distribution.

2. Rayleigh Region

In the Rayleigh region, as $\alpha \rightarrow 0$, $K(\alpha) \sim \alpha^4$

Thus we may write $K(a, \lambda) = K(\alpha_m) \frac{a^4}{a_m^4}$

Then equation 9 becomes

$$K_{\text{eff}} = K(\alpha_m) \int_0^{\infty} \left(\frac{a}{a_m} \right)^6 p(a) da$$

Again, using equation 5, this becomes

$$K_{\text{eff}} = K(\alpha_m) \frac{(\sigma + 5)(\sigma + 4)(\sigma + 3)(\sigma + 2)(\sigma + 1)}{\sigma^5} \quad (17)$$

Proceeding as before,

$$\frac{\Delta I_{\sigma}}{\Delta I_{\delta}} = \frac{(\sigma + 5)(\sigma + 4)(\sigma + 3)}{\sigma^3} \quad (18)$$

In this case, for $\infty > \sigma > 4$, $1 < \frac{\Delta I_{\sigma}}{\Delta I_{\delta}} < 7.87$

We have a sizeable possible error for this case and a complete reversal of it from the previous case; i.e. ignoring the distribution of particle sizes underestimates rather than overestimates the scattering, in contradistinction to the observed behavior in the optical region.

In general, $K(\alpha)$ in the Mie region, is very complicated in shape, and a particular value of a_m and σ may result in particle sizes lying within two regions. Thus, although these limiting cases are of interest and indicate trends with a_m and σ we need numerical solutions to study the complete behavior.

C. A Sample Problem

Of particular interest to crossed beam measurements is the scattering to be expected from water vapor condensing within a turbulent jet at a wavelength near 4.3μ . The jet velocity is obtained by expanding from a compressed air supply, which in turn has a very low absolute humidity since most of the water vapor condenses out during interstage cooling. Water vapor condensation therefore occurs when ambient air is mixed into the cool jet, and we need to know the ambient humidity. For an ambient temperature of 27°C realistic room

dew point is 15°C which corresponds to $\beta \approx .5$ at 760 torr pressure. Crossed-beam studies⁽⁸⁾ at IIT Research Institute are made using a 2.54 cm jet at a typical flow Mach number of $M = .62$. The jet temperature, expanding from an ambient temperature of 27°C is then 4°C. Thus water droplets, not ice crystals are formed. The following conditions were chosen for sample calculations:

$$\begin{aligned}
 d &= .1\text{cm} \\
 L &= 10\text{cm} \\
 \lambda &= .2 \text{ to } 20\mu \\
 M_v &= 18 \\
 M_a &= 29 \\
 \rho_{cj} &= 1.000 \text{ gm/cc at } T_j = 4^\circ\text{C} \\
 \rho_a &= .001177 \text{ gm/cc at } T_a = 27^\circ\text{C} \\
 \nu &= 0.5 \\
 P_a &= 760 \text{ torr} \\
 P_{sa} &= 26.739 \text{ torr at } T_a = 27^\circ\text{C} \\
 P_{sj} &= 6.101 \text{ torr at } T_j = 4^\circ\text{C} \\
 K(\alpha) &= \text{taken from Figure 1.} \\
 \sigma &= 4, 16, 24, \infty \\
 a_m &= 1 \text{ to } 20\mu
 \end{aligned}$$

The results for $\sigma = \infty$, $a_m = 1\mu$ are shown in Figure 3 plotted as $\frac{\Delta I}{I_0}$ vs α . Since $\frac{\Delta I}{I_0} < 10\%$, the exponential of equation 8 may be simplified by the assumption $e^{-y} = 1 - y$ and $\frac{\Delta I}{I_0} \approx \frac{1}{a_m}$ from equation 8 and 10. Thus the results of Figure 3 may be readily extrapolated to other values of a_m .

The effect of shape of the distribution function (σ) can be seen from Figure 4. The curves have been normalized by the value at $\sigma = \infty$. Although σ has a pronounced effect at small α as noted earlier, the absolute value of the scattering drops off rapidly below $\alpha = 1$ (c.f. Figure 3). The result is that we are concerned primarily with $\alpha > 1$ and here the ratio $\frac{\Delta I_\sigma}{\Delta I_\infty}$ lies between 3 and 2/3 for $\sigma > 4$. As a first approximation then, we can ignore the correction for σ and after determining the conditions for maximum scattering, reassess the effect of σ . In Figure 5, $\frac{\Delta I}{I_0}$ is plotted for two values of λ : one corresponds to the CO_2 band center at 4.3μ and the other corresponds to the ultra violet oxygen bands (Schumann-Range) at $.18\mu$. The figure points up clearly the increased effect of peak scattering at small wavelengths. The peak scattering occurs at $a_m = .15\mu$ or $\alpha = 6$ for $\lambda = .18\mu$ and at $a_m = 3.4\mu$ or $\alpha = 5$ for $\lambda = 4.3\mu$. At these values of α , the correction for σ from Figure 3 is less than 40% for $4 < \sigma < \infty$. At $\lambda = 4.3\mu$ the maximum scattering expected for our test case then is about 3% and at $\lambda = .18\mu$ is 65%. Crossed-beam studies are made with $\frac{\Delta I}{I_0} \simeq 50\%$ to give an optimum signal-to-noise ratio. Hence at $\lambda = 4.3\mu$ scattering from water droplets should be negligible but not necessarily so at $\lambda = .18\mu$. This points up the advantage of performing the crossed-beam studies using the infra-red system.

In order to apply these results to experiments at conditions other than those assumed here, a set of extrapolation rules has been prepared and these are discussed in the following section.

D. Extrapolation to Other Flow Conditions

As observed previously, $\frac{\Delta I}{I_0} < 10\%$ and we can approximate the exponential by the assumption $e^{-y} = 1 - y$. Then equations 8 and 10 indicate a linear relation between $\frac{\Delta I}{I_0}$ and $\frac{1}{a_m}$, $\frac{\rho_a}{\rho_{cj}}$, L , and $H = \frac{P_{sa}}{P_a} (\beta - \frac{P_{sj} T_a}{P_{sa} T_j})$. Extrapolation to conditions other than those of the sample calculation then becomes straightforward.

a) To correct for particle size the results of Figure 3 need only be divided by the mean particle radius in microns.

b) To correct for path length L , the results of Figure 3 should be multiplied by $L/10$ with L in cm.

c) The density of condensate is $\rho_{cj} = 1$ gm/cc to within 2% accuracy from 0°C to 70°C . Consequently the main correction in $\frac{\rho_a}{\rho_{cj}}$ is for ρ_a . Since $\rho_a = .001177$ gm/cc (at $T_a = 300^\circ\text{K}$ and $P_a = 760$ torr) was used in the sample calculation we can correct for ambient air density by multiplying the results of Figure 3

by $\frac{P_a}{760} \times \frac{300}{T_a} = .395 \frac{P_a}{T_a}$, where P_a is in torr, T_a in $^\circ\text{K}$.

d) The remaining correction is really a correction for T_a and T_j . Thus to correct for humidity effects, H can be calculated from P_{sa} and P_{sj} (determined from Reference 6 and plotted as in Figure 6) and the known value of β . Since $H = 9.574 \times 10^{-3}$ for the sample calculation, the results of Figure 3 should then be multiplied by $\frac{H_{\text{actual}}}{9.564 \times 10^{-3}}$.

IV. EXPERIMENTAL STUDIES

Single beam autocovariance measurements were taken using the beam-splitter arrangement⁽⁹⁾ on the infra-red system, at a downstream location of 4 jet diameters. The beam-splitter arrangement gives a measurement independent of electronic and detector noise. The reading obtained is of course the mean-square fluctuating signal and we are interested in comparisons with the extinction of the mean signal. To accomplish such a comparison we must make some assumptions concerning the statistical behavior and interdependency of the scattering and absorbing signals.

A. Relation of Measured Signals to Mean Extinction

It has already been assumed that the scattering particles are completely mixed within the jet by the action of turbulence. If it is assumed that density gradients are mixed in the same way, we would expect the statistical behavior of scattering and absorption to be identical and we will make such an assumption here.

Let i_s , i_a be the instantaneous a.c. signals from scattering and absorption and ΔI_s and ΔI_a be the corresponding mean signal extinctions

$$\text{then } i = i_s + i_a \quad (19)$$

and

$$\langle i^2 \rangle = \langle (i_s + i_a)^2 \rangle = \langle i_s^2 \rangle + \langle i_a^2 \rangle + \langle i_s i_a \rangle \quad (20)$$

Since the mixing processes are taken identical for scattering and absorption

$$\frac{\langle i_s^2 \rangle}{\Delta I_s^2} = \frac{\langle i_a^2 \rangle}{\Delta I_a^2} = \frac{\langle i_s i_a \rangle}{\Delta I_a \Delta I_s} \quad (21)$$

Then

$$\frac{\langle i_s^2 \rangle}{\langle i^2 \rangle} = \frac{\Delta I_s^2}{\Delta I_s^2 + \Delta I_a^2 + \Delta I_a \Delta I_s} \equiv s^2 \quad (22)$$

from which

$$\frac{\Delta I_s}{\Delta I_a} = \frac{1 \pm \sqrt{1 + 4\left(\frac{1}{s^2} - 1\right)}}{2\left(\frac{1}{s^2} - 1\right)} \quad (23)$$

The + sign holds where scattering dominates (in wings of band) whereas the - sign holds where absorption dominates (in band center).

The ratio s^2 is measurable with the infra-red system by making measurements in the 4.3μ band and obtaining $\langle i^2 \rangle$ and then taking measurements off-band where only scattering should exist, and obtaining $\langle i_s^2 \rangle$. Early results with the infra-red system showed evidence of oil particles causing scattering but this problem has since been alleviated and it is believed, is no longer a problem.⁽¹⁰⁾ The total absorption extinction ΔI_a is measured by taking d.c. intensity readings across the 4.3μ band and correcting for that portion of the path which does not pass through the jet. It is assumed that $\Delta I_s \ll \Delta I_a$ and can be neglected in this measurement. This limits us to the - sign solution of equation (23). Such measurements are reported in the next section.

B. Observations

Profiles for $\langle i^2 \rangle$, I and ΔI_a taken across the 4.3_μ band are reproduced in Figure 7. The estimated value for $\langle i_s^2 \rangle$ was assumed constant in the calculation of s^2 . The ratio $\frac{\Delta I_s}{\Delta I_a}$ was calculated from equation 23 (using the minus sign) and the estimate of $\frac{\Delta I_s}{I_o}$ determined (See figure 8). Thus the experiment indicates that the mean extinction due to scattering is about 6% of the light incident intensity i.e. $\frac{\Delta I_s}{I_o} \simeq .06$ in the center of the band.

The actual condition for the experiment were $T_a = 29^\circ\text{C}$, $T_j = 4^\circ\text{C}$, $\beta = .4$, $M = .62$. The dew point occurs at $T_d = 19^\circ\text{C}$. If we assume the stagnation temperature constant, equal to T_a throughout the jet, then we can use the local isentropic relation to calculate the local speed.

$$\text{i.e. } \frac{273 + T_a}{273 + T_d} = \frac{302}{292} = 1 + 0.2 M^2 \left(\frac{U(y/D)}{U(o)} \right)^2$$

where $U(y/D)$ is the speed at the radial position y/D where $T = T_d$ and $U(o)$ is the center-line speed. This gives $\frac{U(y/D)}{U(o)} = .62$, which occurs⁽¹¹⁾ at $y = D/2$. Thus the width of jet of interest, $L = 2y = D = 2.54$ cm, instead of $L = 10$ cm as used in Figure 3 and we must correct the results (using extrapolation procedure b) of Section III D) by a factor of $\frac{2.54}{10} \simeq \frac{1}{4}$.

The correction for $\frac{\rho_{cj}}{\rho_a}$ is less than 1% and will be ignored. However a correction is required for H in order to use Figure 3. From Figure 6, taking $T_a = 29^\circ\text{C}$, $T_j = 19^\circ\text{C}$, we obtain $\frac{P_{sa}}{P_a} = .04$ and $\frac{P_{sj}}{P_a} = .021$ then $H = .04(.4 - .021 \times \frac{302}{292}) = .0076 = 7.6 \times 10^{-3}$. The correction (using the extrapolation procedure c) of Section III D) then is $\frac{7.6 \times 10^{-3}}{9.6 \times 10^{-3}} \approx 0.8$ and the total correction is $\frac{0.8}{4} = .2$. The experimental measurement indicates that $\Delta \frac{I_s}{I_o}$ is about .06, under the condition tested. If the conditions had been those of the sample problem, we would have obtained a measured $\frac{\Delta I_s}{I_o} = \frac{.06}{.2} = .30$. This number is much higher than the maximum value $\frac{\Delta I_s}{I_o} = .03$ shown in Figure 5 at 4.3μ and would lead us to the conclusion that water vapour condensate is not sufficiently large to account for the off-band signal.

V. DISCUSSION

The analysis presented here, designed to give a maximum estimate, predicts that scattering from condensed water droplets should be no problem at $\lambda = 4.3\mu$. Experimentally, however, we find that scattering levels, although not dominant, are an appreciable fraction of the total signal. Although the estimates, both analytical and experimental are rough, accuracy is sufficiently good that we must conclude that there is scattering occurring from particles other than water droplets. Earlier studies showed that oil droplets in the IITRI facility dominated the scattering signal, and although this has been reduced, it would appear that it still amounts to at least an order of magnitude more signal than can be expected from water vapor condensate.

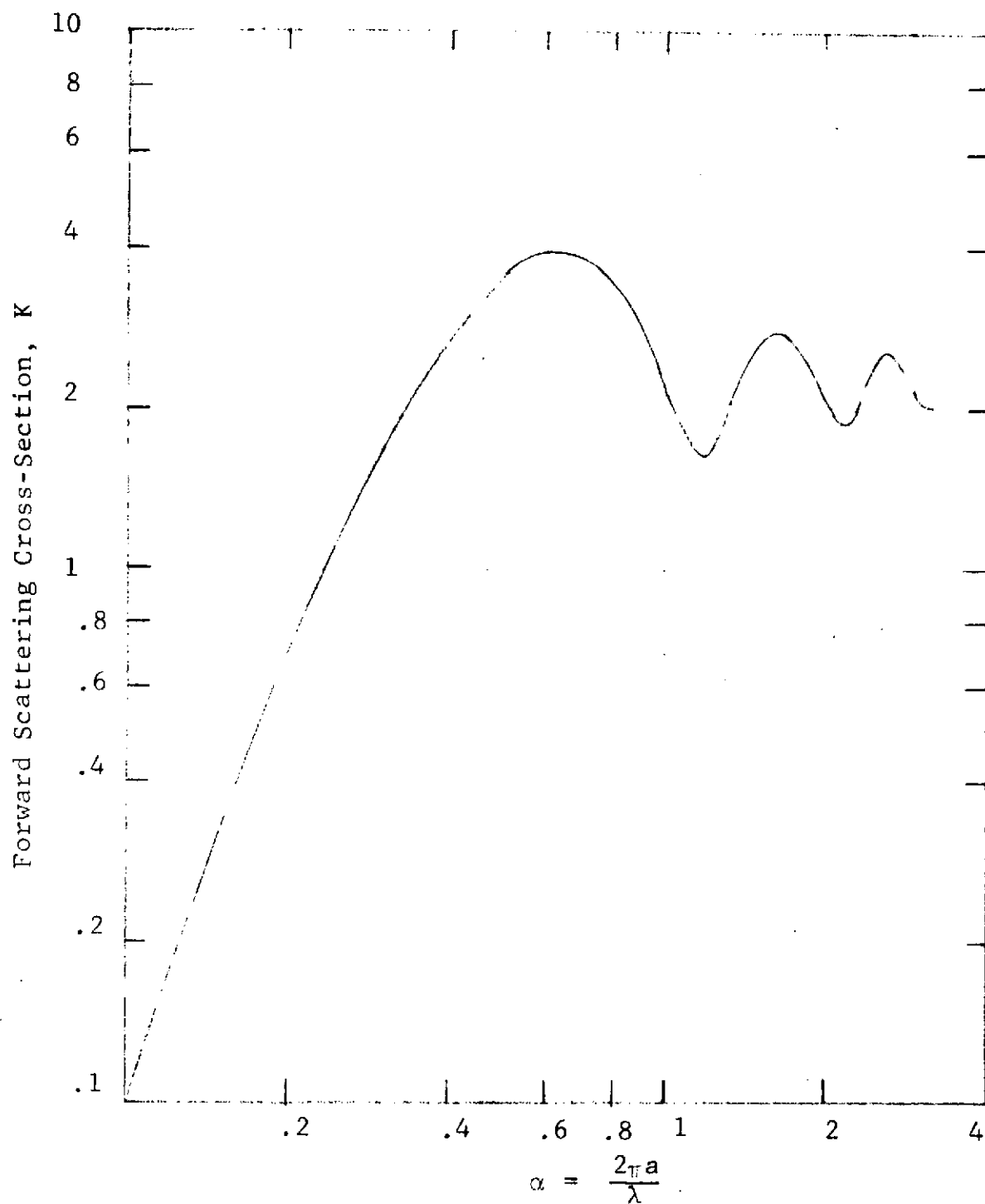


Figure 1 CROSS SECTIONS FOR FORWARD SCATTERING FROM SPHERICAL WATER DROPLETS.

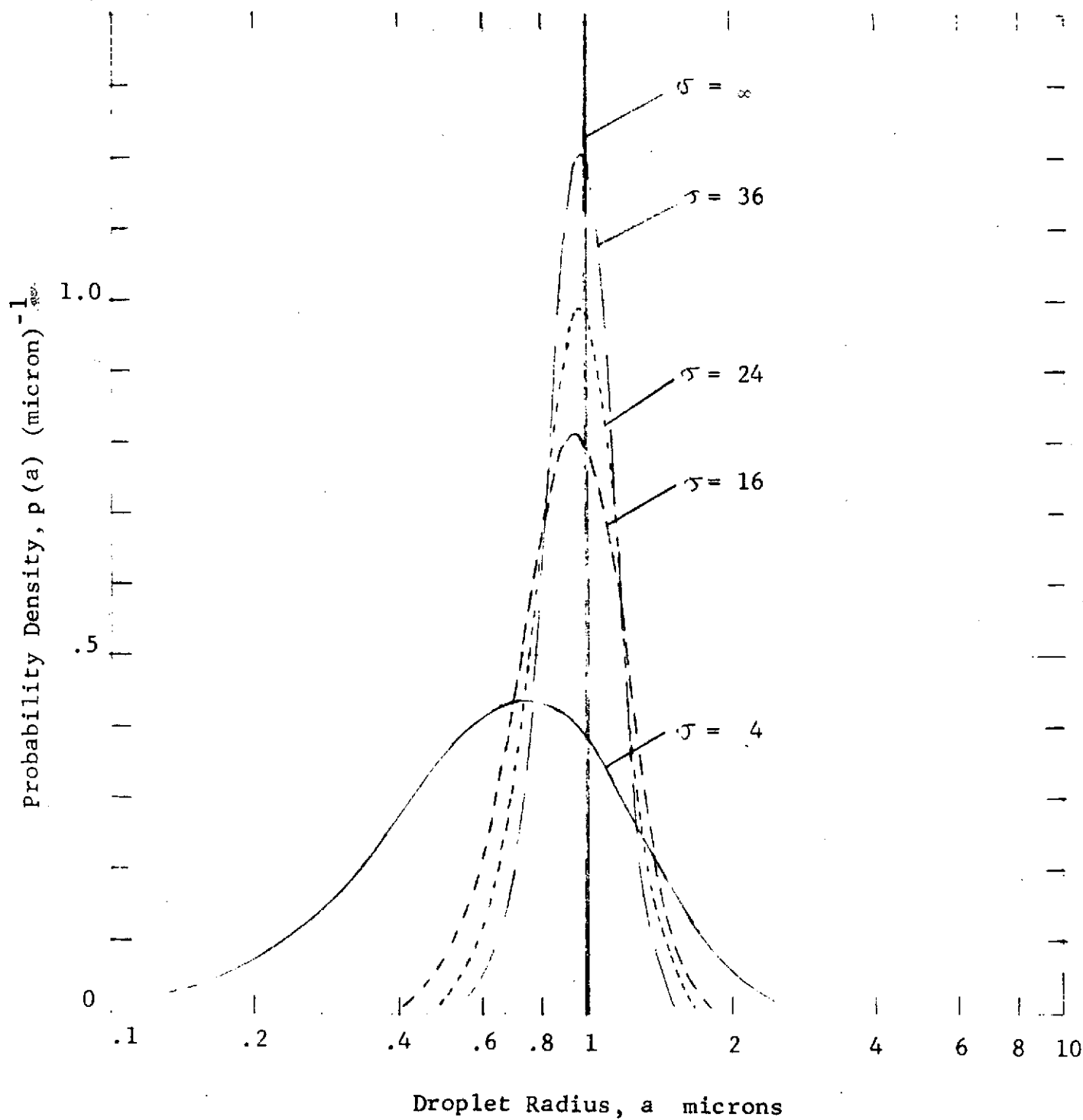


Figure 2 GAMMA PROBABILITY DISTRIBUTION FOR MEAN DROPLET RADIUS $a_m = 1$ MICRON.

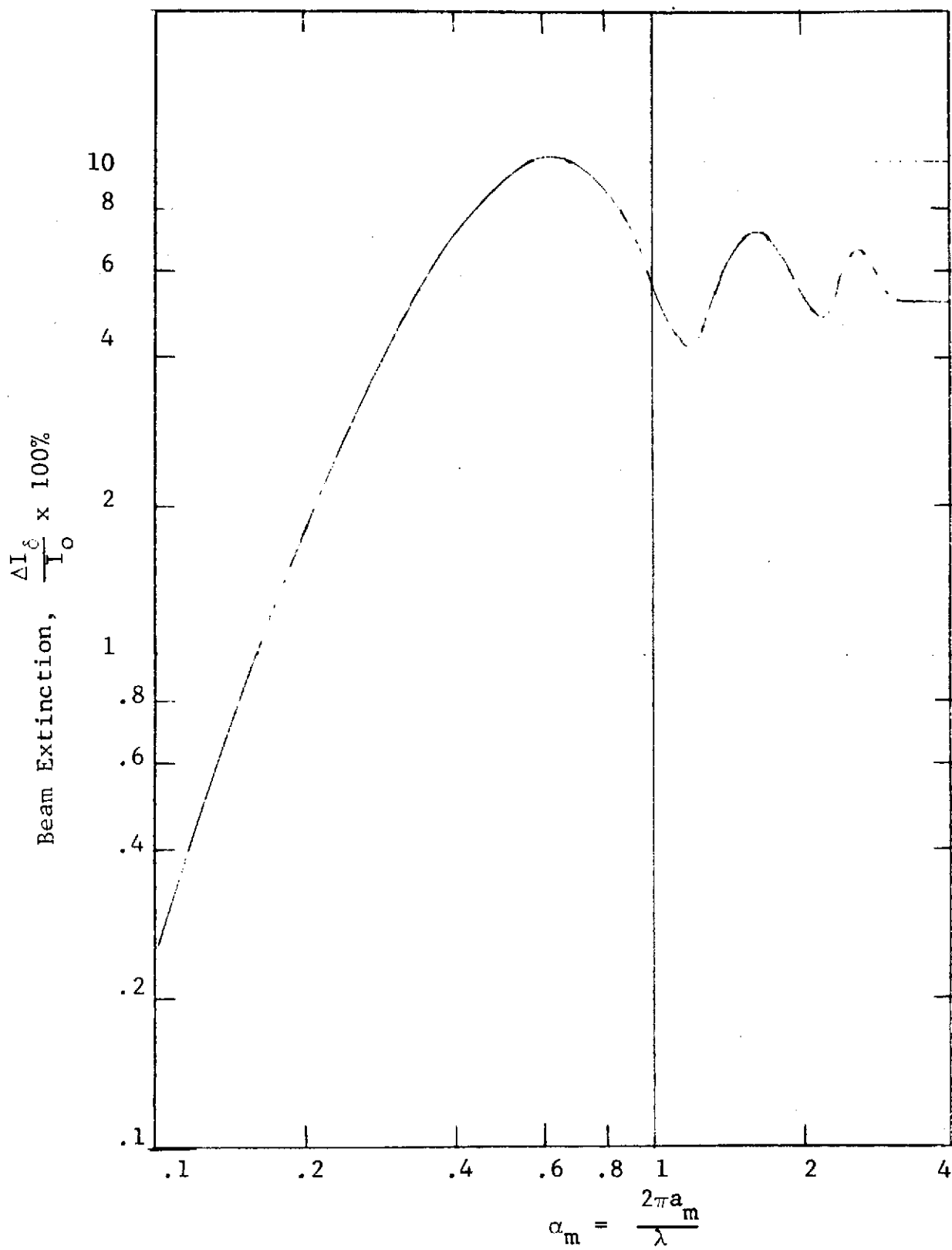


Figure 3 BEAM EXTINCTION FOR SAMPLE PROBLEM
 δ - FUNCTIONAL DISTRIBUTION.

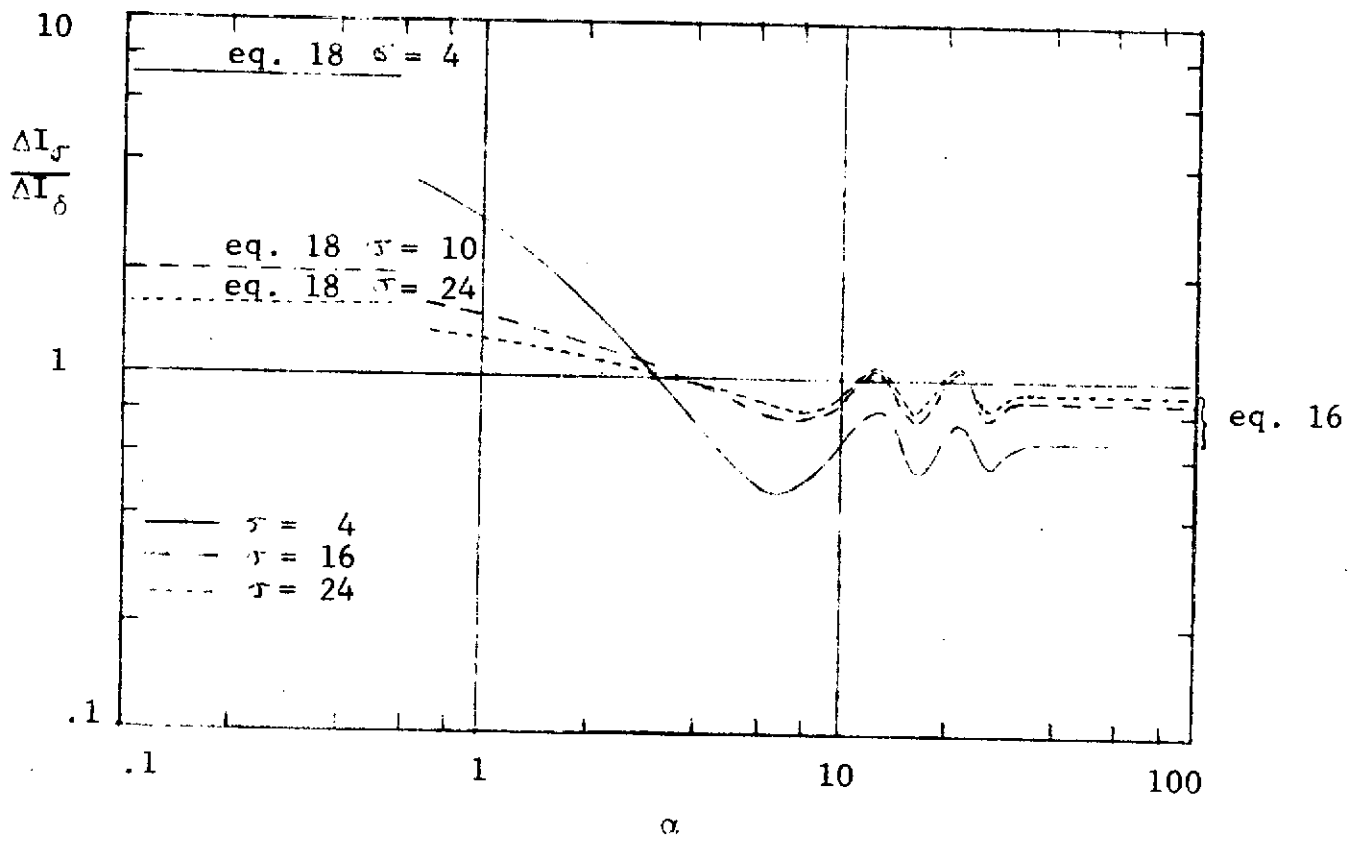
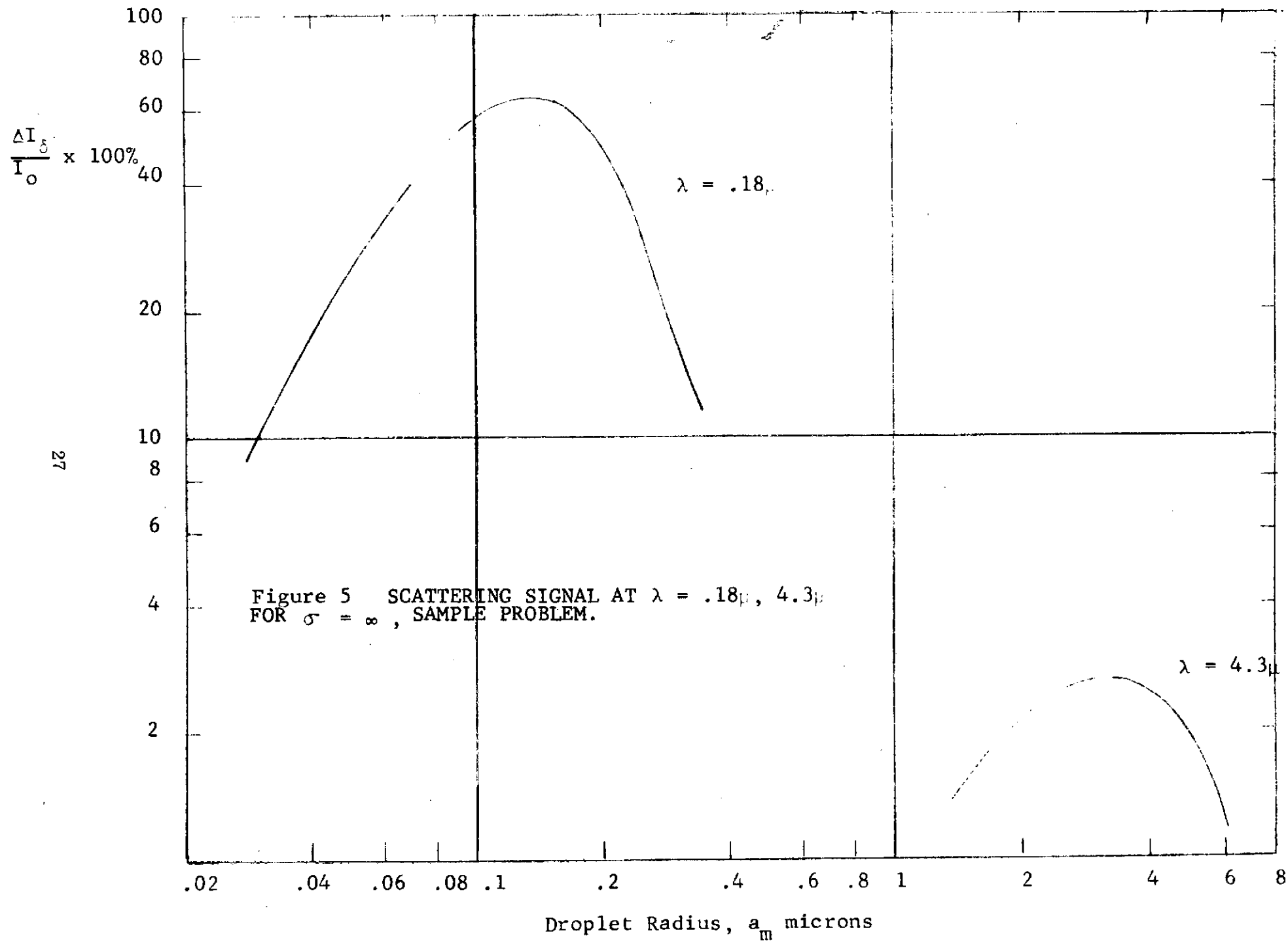


Figure 4 EFFECT OF PARTICLE SIZE DISTRIBUTION FOR SAMPLE PROBLEM.



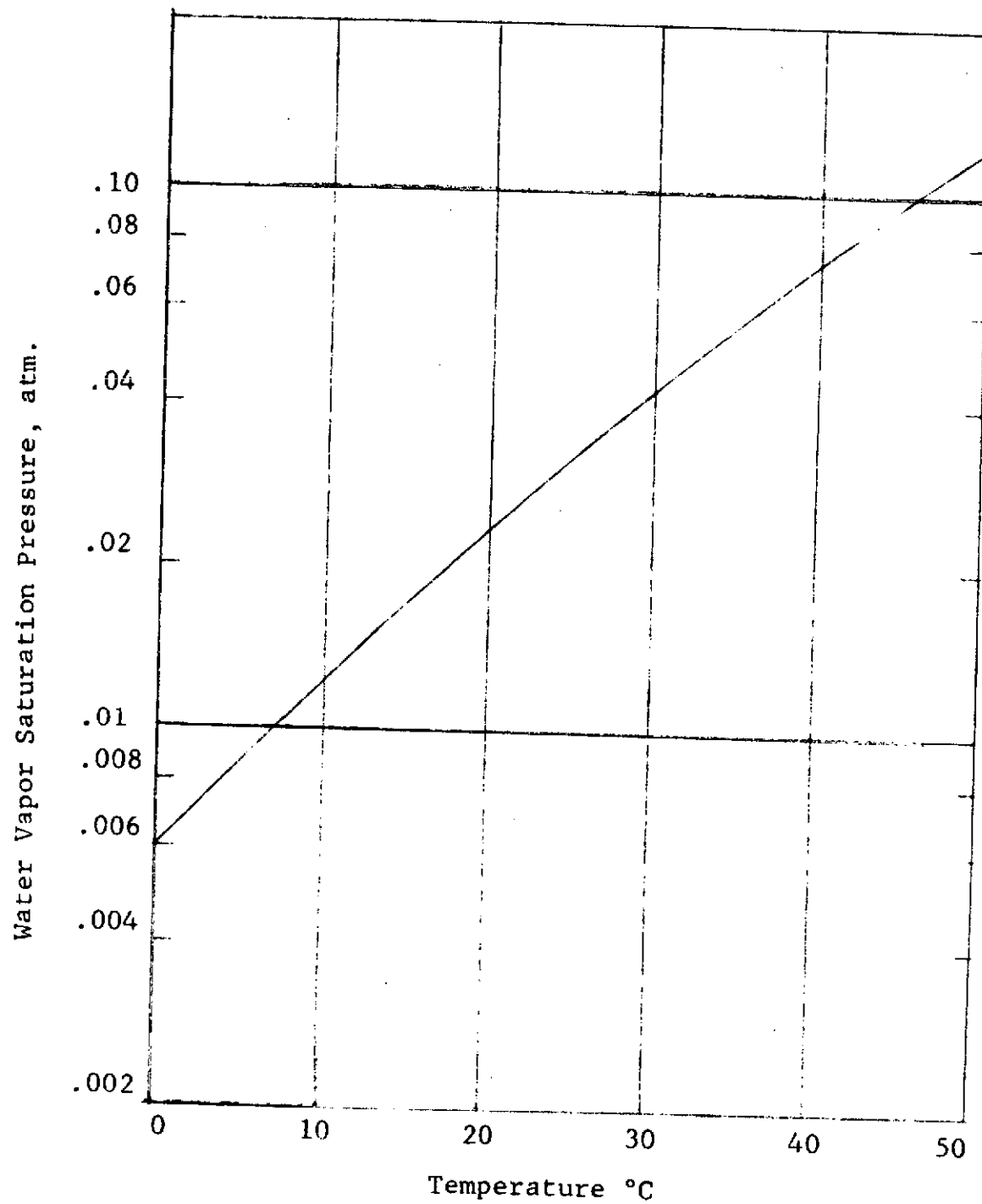


Figure 6 WATER VAPOR SATURATION PRESSURES

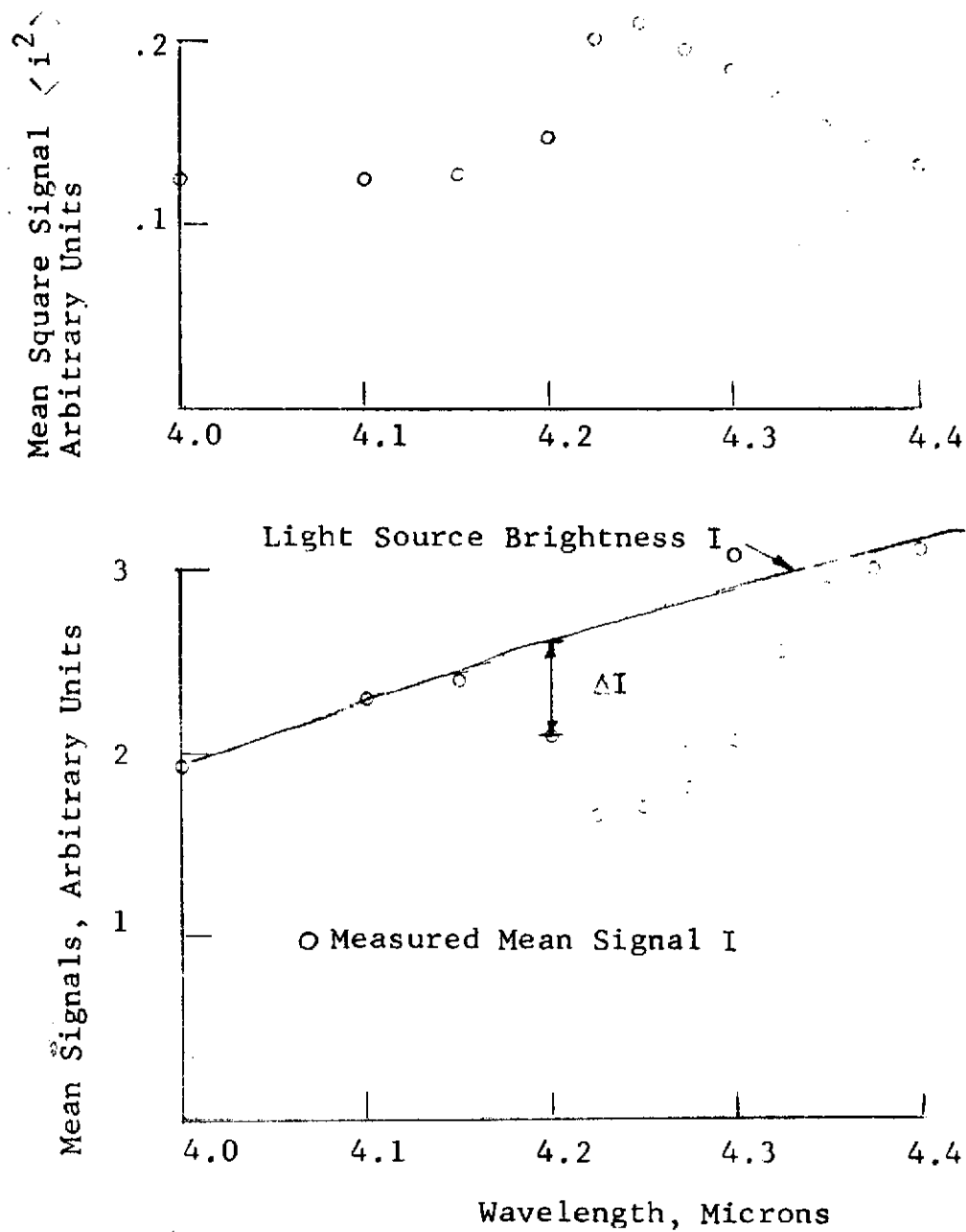


Figure 7 MEASURED MEAN AND FLUCTUATING SIGNALS FROM I.R. SYSTEM.

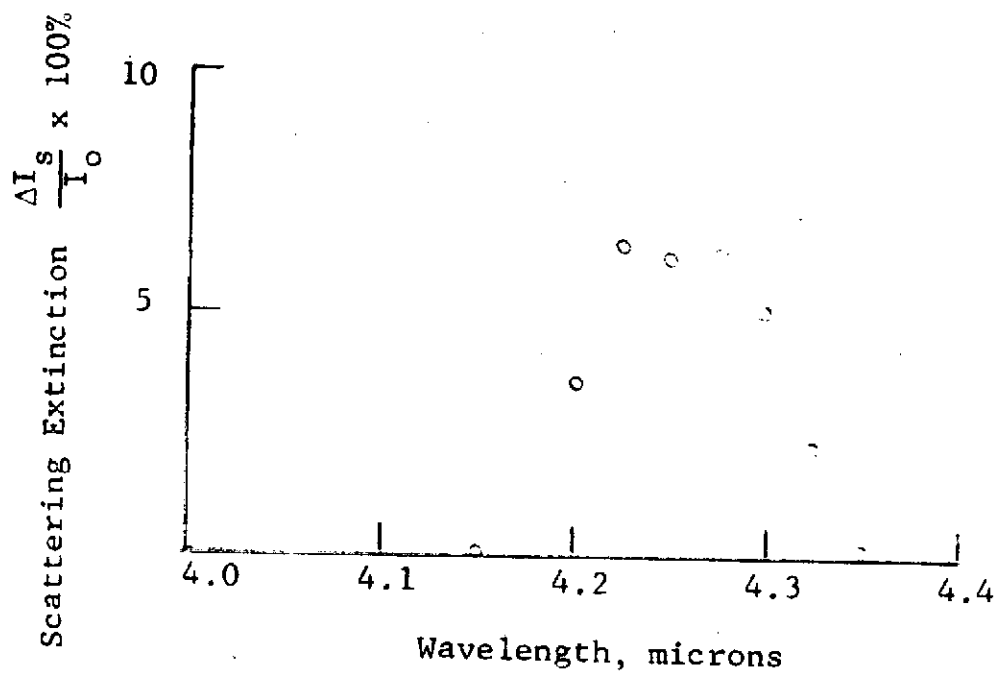


Figure 8 MEAN SCATTERING SIGNAL CALCULATED FROM EXPERIMENTAL MEASUREMENTS.

REFERENCES

1. Fisher, M. J. and Damkevala, R. J., Shock Wave Shear Layer Interaction in Clustered Rocket Exhaust, IITRI Final Report on Contract No. NAS 8-20408, October 1967.
2. Krause, F. R. and Wilson, L. N., "Optical Crossed-Beam Investigation of Local Sound Generation in Jets", NASA SP-189, (1968).
3. Born, M. and Wolf, E., Principles of Optics, Pergamon Press, New York (1959).
4. Goldberg, B., J. Opt. Soc. Amer., 43, (1953) 1221
5. Abramowitz, M., and Stegun, L. A., ed. "Handbook of Mathematical Functions", page 930, NBS Applied Math. Series 55, (1964).
6. Handbook of Chemistry and Physics, Chemical Rubber Publishing Co., Cleveland.
7. Denman, H. H., Heller, W. and Pangonis, W. J., Angular Scattering Functions for Spheres, Wayne State University Press, Detroit, Michigan, 1966.
8. Wilson, L. N., Krause, F. R. and Kadrmas, K., "Optical Measurements of Sound Source Intensity in Jets", NASA Conference on Basic Noise Research, NASA SP 207, (1969).
9. Damkevala, R. J., Crossed Beam Instrument Mk II Operation Manual, IITRI Final Report on Contract No. NAS 8-21035, 1970.
10. Damkevala, R. J., Calibration Report, IITRI Final Report on Contract NAS 8-24407, 1970.
11. Davies, P. O. A. L., Fisher, M. J., and Barratt, M. J., "The Characteristics of the Turbulence in the Mixing Region of a Round Jet", J. of Fluid Mech., 15, 337 (1963).